



# Detection of oral mucosal lesions by the fluorescence spectroscopy and classification of cancerous stages by support vector machine

Pavan Kumar<sup>1,2</sup> · Shashikant Rathod<sup>1,3</sup> · Asima Pradhan<sup>2</sup>

Received: 25 August 2023 / Accepted: 12 January 2024

© The Author(s), under exclusive licence to Springer-Verlag London Ltd., part of Springer Nature 2024

## Abstract

Detection of oral mucosal lesions has been performed by an in-house developed fluorescence-based portable device in the present study. A laser diode of 405 nm wavelength and a UV-visible spectrometer are utilized in the portable device as excitation and detection sources. At the 405 nm excitation wavelength, the flavin adenine dinucleotide (FAD) band at 500 nm and three porphyrin bands at 634, 676, and 703 nm are observed in the fluorescence spectrum of the oral cavity tissue. We have conducted this clinical study on a total of 189 tissue sites of 36 oral squamous cell carcinoma (OSCC) patients, 18 dysplastic (precancerous) patients, and 34 volunteers. Analysis of the fluorescence data has been performed by using the principal component analysis (PCA) method and support vector machine (SVM) classifier. PCA is applied first in the spectral data to reduce the dimension, and then classification among the three groups has been executed by employing the SVM. The SVM classifier includes linear, radial basis function (RBF), polynomial, and sigmoid kernels, and their classification efficacies are computed. Linear and RBF kernels on the testing data sets differentiated OSCC and dysplasia to normal with an accuracy of 100% and OSCC to dysplasia with an accuracy of 95% and 97%, respectively. Polynomial and sigmoid kernels showed less accuracy values among the groups ranging from 48 to 88% and 51 to 100%, respectively. The result indicates that fluorescence spectroscopy and the SVM classifier can help to identify early oral mucosal lesions with significant high accuracy.

**Keywords** Oral lesions · Fluorescence spectroscopy · Fluorophores · Principal component analysis · Support vector machine · Kernels

## Introduction

An increase in the rate of oral cavity malignancy worldwide, especially in Asian countries, is a serious issue and a challenge to the scientific community and government. According to the report, the incidence rate of oral cancer will rise and is expected to reach 1.7 million in 2023. Worldwide, oral cancer is the sixth most common cancer. In India, it is ranked number one and therefore a significant public health importance. The primary causes of the high incidence and

death rates in India are a lack of awareness of its severity, inadequate access of trained providers, and limited health facilities. Diagnostic faculties/treatment available in clinics is not affordable by most of the Indian population because of their low capital income. Studies revealed that a 5-year survival rate is considerably less (~45%) and has not improved in the last few decades. The cause of poor survivability is late diagnosis and absence of early symptoms. There is a higher chance to cure the disease by detecting it at an early stage. Moreover, it is possible to reduce the incident and death rates. To overcome the morbidity and mortality rates, non-invasive sensitive devices and machine learning-based tools are needed, which could discern among the groups with greater accuracy values [1–3].

Visual inspection, brush biopsy, toluidine blue, histopathology, etc., are some of the conventional techniques to detect the oral lesions. Among the traditional methods, tissue biopsy with histopathological examination is one of the reliable or the gold standard tool for the detection of oral cavity lesions. The major complication with biopsy-based

✉ Pavan Kumar  
pavan2012iitk@gmail.com

<sup>1</sup> Faculty of Engineering and Technology (FEAT), Datta Meghe Institute of Higher Education and Research (DMIHER), Wardha 442001, India

<sup>2</sup> Department of Physics, Indian Institute of Technology Kanpur (IITK), Kanpur 208016, India

<sup>3</sup> Department of Instrumentation and Control Engineering, COEP Technological University, Pune 445001, India

tool is their invasive way of treatment. All patients with the abnormality, whether benign, dysplastic (mild, moderate, severe), or OSCC (Stages I to IV) must undergo this painful process during the treatment. Sometimes, patients must go through multiple biopsies to identify the right abnormal area/part of tissue [4–6]. To overcome these complications, there is a need for such tools which could locate the abnormal lesions non-invasively. Several non-invasive optical techniques such as fluorescence spectroscopy and imaging, Raman spectroscopy and imaging, and diffuse reflectance (DR) spectroscopy and imaging have been adopted by many research groups and clinicians to identify the various lesions [7–17]. Among the optical techniques, fluorescence-based devices (spectroscopic and imaging) are extensively used by many researchers for in vivo detection of oral cancer [18–33]. Other alternatives such as body fluids (saliva, blood, urine, etc.) have also been studied for the detection of oral mucosal lesions by the research groups [34–37]. Various biomarkers or fluorophore molecules are found in human oral cavity tissue. Fluorophores with emission bands near the UV or in visible ranges are tryptophan ( $\lambda_{\text{emi}} = 340$  nm), collagen ( $\lambda_{\text{emi}} = 390$  nm), nicotinamide adenine dinucleotide (NADH;  $\lambda_{\text{emi}} = 440$  nm), flavin adenine dinucleotide (FAD;  $\lambda_{\text{emi}} = 530$  nm), and porphyrins ( $\lambda_{\text{emi}} = 634$  nm). It is established that biochemical and morphological changes occur with the progress of disease in the tissue of the oral cavity. Studies report that with the progress of cancer, the concentration of NADH and porphyrin enhances and FAD contribution decreases [26–28]. Studies conducted by the researcher groups for the detection oral cancer using the optical techniques are summarized briefly and mentioned in the paragraph below.

Red fluorescence was first identified by the Policard in the malignant tumors as being from porphyrins in a rat sarcoma using a Wood's lamp [22]. A clinical work conducted by Inaguma M and Hashimoto K group for the detection of oral carcinoma using an in-house developed near-UV excited autofluorescence diagnosis (NEAD) system found that 85% of carcinoma patients showed porphyrin-like fluorescence when exposed to 405 nm light [23]. Gillenwater et al. performed a clinical study using a fluorescence spectroscopy system (excitation wavelength = 337 nm) on normal, dysplastic, and malignant oral mucosa and estimated that the ratio of intensities of red to blue regions was greater in abnormal areas. They achieved sensitivity and specificity values of 88% and 100%, respectively [24]. Majumder et al. group performed a pilot study for the detection of oral carcinoma using the fluorescence spectroscopy-based device. They showed that oral carcinoma could be differentiated to normal with 86% sensitivity and 63% specificity [25]. Lane et al. group utilized a handheld device based on fluorescence for the visualization of oral lesions. They could differentiate the normal mucosa to invasive carcinoma with sensitivity and specificity of 98% and 100%, respectively

[26]. An anatomy-based study was conducted by Diana C.G. de Veld on healthy oral mucosa and observed variation in fluorescence intensities in oral mucosal sites [27]. A comparative evaluation was done by the Jayanthi et al. group for the detection of oral mucosal lesions by utilizing autofluorescence (AF) and diffuse reflectance (DR) spectroscopy systems. They achieved AUC-ROC values of 0.987 for AF and 0.991 for DR spectroscopy techniques, respectively [28]. Tobacco abuse in the oral mucosa was studied by the Nazeer et al. group using the fluorescence spectroscopy on different groups. Using the multivariate analysis (PCA-LDA), they found sensitivity values in between 60 and 100% and specificity values in between 76 and 100% for discriminating of habitues, non-habitues, and leukoplakia [29].

In the present study, in vivo detection of oral mucosal lesions using an in-house developed fluorescence-based device/probe has been executed. Measurements are conducted on oral squamous cell carcinoma (OSCC) patients, dysplastic patients, and the healthy volunteers of various age groups. FAD and porphyrin bands are observed in the recorded fluorescence spectra. In OSCC and dysplastic patients, porphyrin fluorescence is more common than in the healthy group. To differentiate among the cancerous stages, i.e., OSCC to dysplasia, dysplasia to normal, and OSCC to normal, statistical tools such as principal component analysis (PCA) and support vector machine (SVM) classifier are employed. The SVM classifier incorporates various kernels such as linear, radial basis function (RBF), polynomial, and sigmoid. To our knowledge, a detailed comparison by including the different kernels in the SVM classifier for the discrimination among the groups has yet to be reported for oral mucosal lesions.

## Materials and methods

### Instrumentation and data collection

Fluorescence data were collected from 79, 48, and 62 tissue sites of 36 OSCC patients, 18 dysplastic patients, and 34 normal volunteers. The mean age of the patients (OSCC and dysplastic) and control group with the standard deviation was  $45 \pm 11$ ,  $36 \pm 7$ , and  $34 \pm 6$ , respectively. Patients who visited to hospital for the treatment were instructed to avoid food and beverages altogether. They were also advised to rinse their oral cavity. We observed that most of the patients reported for treatment had few common habits like chewing of tobacco, tobacco-based pan masala, smoking bide, and consumption of alcohol (infrequently). The control group selection was restricted to only those who were free from any disease and habits. Patients having the symptoms, e.g., whitish patches, red patches, a combination of white and red patches, and raised growth, were included. A very few

patients who displayed some signs of ulcer and infection were excluded from the abnormal group after capturing the fluorescence data with the consult of doctors. The spectral profile of such patients was similar to the spectral profile of the control group. After recording the data, patients were sent for oral biopsy. A small specimen was taken out from the abnormal area of oral cavity and sent for histopathology. As per the outcome of the histopathology report, treatment has been accomplished by the clinicians. Most of the reported patients have to go through the surgery. In this process, all the abnormal area of the oral cavity was removed. Other medications were also taken care of by the clinicians throughout the treatment. For the spectroscopic data analysis, histopathology data were bifurcated into different groups.

We conducted the fluorescence measurements on patients (OSCC and dysplasia) and normal volunteers by an in-house developed handheld device (fabricated in the CELP workshop at IIT Kanpur, India). The device was installed in Hallet Hospital of GSVM Medical College Kanpur, Uttar Pradesh, India, for clinical testing. The device consists of a 405 nm diode laser, two collimating lenses (CL), a beam splitter (BS), a long pass filter (450 nm), connecting fibers, and a spectrometer. A schematic diagram with the photograph of the device and other required accessories while recording data on a patient is shown in Fig. 1a and b, respectively. Laser light is shone on the oral cavity tissue, and the fluorescence signal is recorded using the UV-visible spectrometer. Ocean Optics Spectra Suit Software is used for data acquisition. Spectra recorded from abnormal and normal areas of a patient's oral cavity are displayed in Fig. 1b. Porphyrin content (634 nm) is found much higher in the abnormal area than in the normal area of the oral cavity. It indicates that the device can detect and differentiate between the normal and abnormal parts of the oral tissue. A disposable cap of Teflon material (Virgin PTFE) is used at the device's tip. Its size was designed in such a way that focused light irradiate at the tip of the cap. The cap's design was done in the CELT workshop, at IIT Kanpur, India. Since the focused incident light

at the surface of any material gives maximum fluorescence signal, therefore the cap's length was arrested according to the lens focal length. The spot size of the focused light was  $\approx 1$  nm. With this arrestment, we obtained excellent spatial resolution. Optimal powers of 122  $\mu$ W and integration time of 3 s were significant enough to record the fluorescence signal from oral cavity sites.

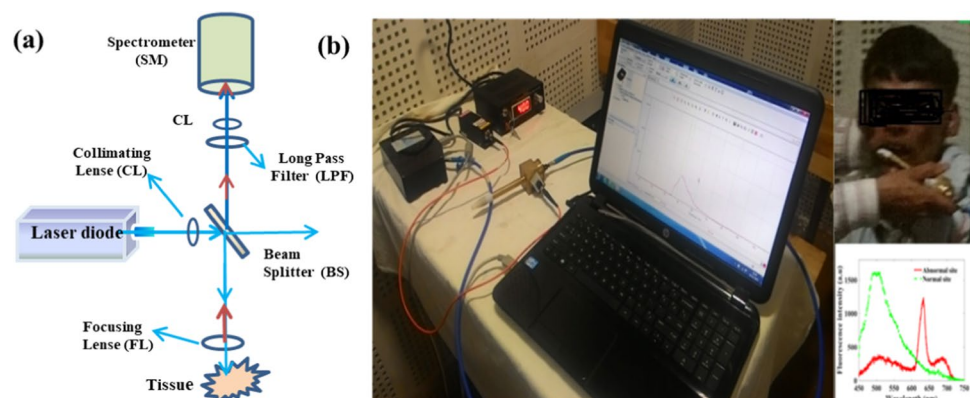
### Follow-up of ethical approval

To conduct the clinical study, we had taken the ethical approval from the committee members of IIT Kanpur, UP, India, and GSVM Medical College, UP, India. We obtained ethical clearance with IEC communication number IITK/IEC/2015-16/2/10. We also got approval from the Clinical Trials Registry-India (CTRI) and received the approval with registration number CTRI/2017/10/010102. Patients and volunteers reported in the hospital for the cancer diagnosis were explained briefly about the working of the device and its advantages over the biopsy. After that, informed consent was taken from the admitted patients. In a questionnaire, we noted personal and professional details such as age, background of family, lifestyle, occupation, and consuming of unhealthy products.

### Analysis methods (PCA, SVM, and ROC)

In the analysis methods, we employed principal component analysis (PCA), support vector machine (SVM) classifier, and receiver operating characteristic (ROC) analysis. PCA is used on the fluorescence data set to reduce its dimension without losing the information. Dimension reduction can be made by simply computing the eigenvectors, also called principal components. However, SVM is utilized to classify among OSCC, dysplastic, and normal groups. SVM applied on a data set finds an optimal hyperplane that separates data points of different groups. It achieves this classification among the group by maximizing the margin between the decision boundary (hyperplane) and the support

**Fig. 1** **a** Schematic diagram of the fluorescence-based in-house portable device. **b** Photograph of a device with the required accessories such as a hand-held device, laser diode, spectrometer, and laptop, while collecting the data from an oral carcinoma patient



vectors (data points closest to the decision boundary). In the SVM classifier, the most widely used kernels such as linear, radial basis function (RBF), polynomial, and sigmoid were included, and diagnostic parameters such as accuracy, sensitivity, and specificity were computed [37–40]. All the steps included for the classifying of three groups are summarized in the flow chart and displayed in Fig. 2. ROC is used to find the discrimination line and to compute the diagnostic parameters. MATLAB software (MATLAB R2016a, Math-Works, MA, USA) and Python (version 3.9) are utilized to analyze the data.

## Results and discussion

### Fluorescence spectra of buccal mucosa

Typical fluorescence spectra recorded from oral squamous cell carcinoma (OSCC) patients, dysplastic patients, and the control group (normal volunteers) are displayed in Fig. 3a–c. Fluorescence spectra are taken at an excitation wavelength of 405 nm from oral buccal mucosa in the scan range of 450 to 750 nm. Typical fluorescence spectra of three OSCC patients are shown in Fig. 3a by the solid line, dash line, and dash-dot lines, respectively. Similarly, spectra are shown in Fig. 3b and c for dysplastic patients and normal volunteers. In the spectra of all three groups, the presence of an FAD band near 500 nm is observed. However, three porphyrin

bands at 634, 676, and 703 nm are observed in OSCC and dysplastic groups. In the control group, only a minor band at 634 nm is seen (Fig. 3c). OSCC patients’ spectra displayed in Fig. 3a show two types of spectral profiles. In OSCC patient 1, the intensity of the FAD band is much higher than the porphyrin band (634 nm). However, in patients 2 and 3, the intensity of the porphyrin band is higher than that of the FAD bands. In the majority of the OSCC patients ( $\approx 85\%$ ), we found the presence of porphyrin bands. In more than half of the cases, the intensity of porphyrin bands was much higher than the FAD band. Like the OSCC spectra, dysplastic patients’ spectra shown in Fig. 3b consist of two different spectral profiles. In dysplastic patients 1 and 2, the intensity of FAD bands is slightly higher than the porphyrin bands. In patient 3, the intensity of the porphyrin band is larger than the FAD band. In most of the dysplastic patients (70%), we found the presence of porphyrin bands, and in some cases ( $\approx 30\%$ ), porphyrin bands were dominating over the FAD band. In the spectra of the control group, two types of spectral profiles are shown. In normal volunteers 1 and 2, the presence of the FAD band can be seen only. However, FAD and porphyrin bands can be seen in normal volunteer 3. In most of the cases (99%), we only found the presence of FAD band. Only in two volunteers out of 36, a very weak band of porphyrin at 634 nm is seen. These bands may be due to bacterial infections. A typical spectra of a cancerous patient (highly addicted to tobacco-based products), a habituated volunteer (consuming tobacco-based products

**Fig. 2** Steps to classify among the groups using PCA and SVM on fluorescence data of all the three groups

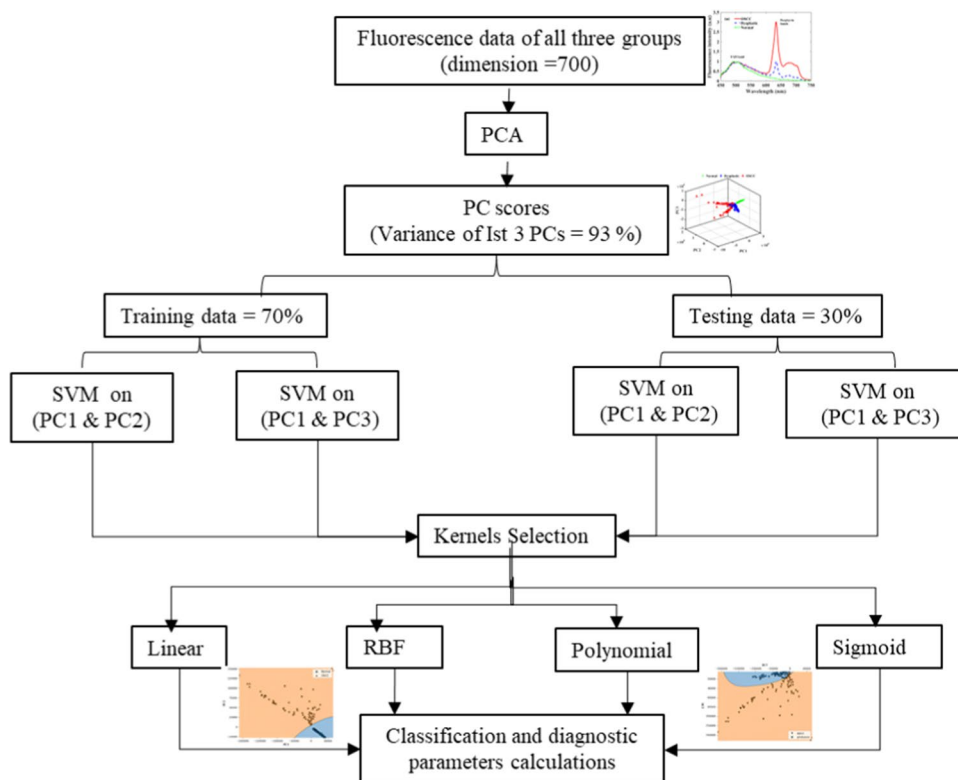
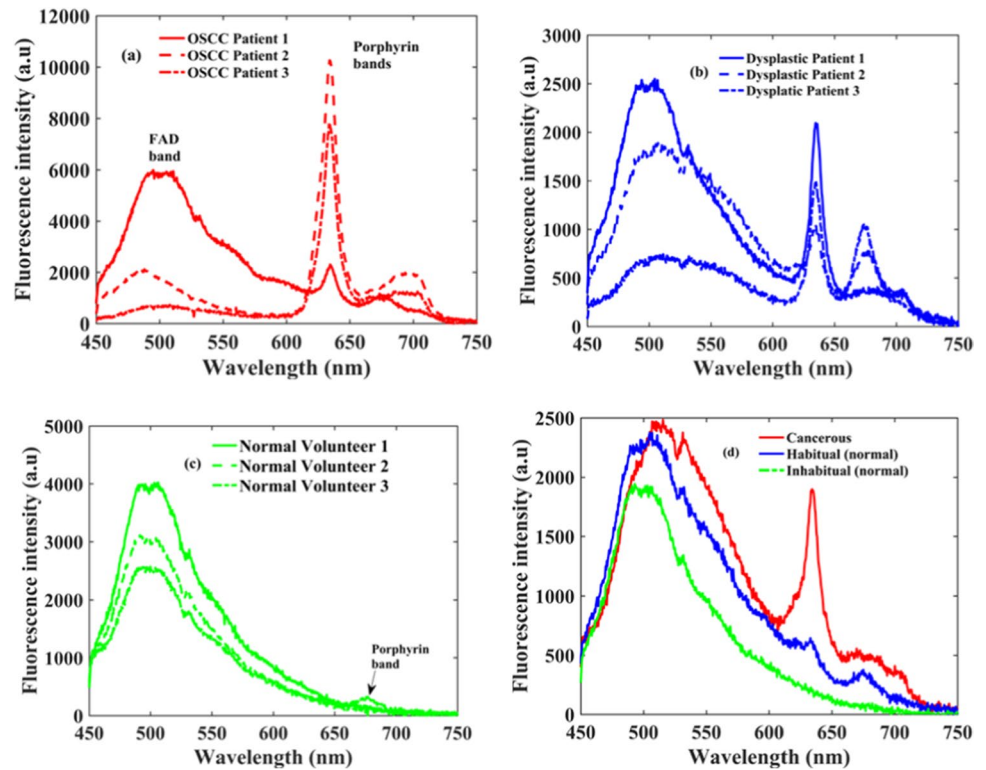




**Fig. 3** **a** Typical fluorescence spectra of three OSCC patients, **b** typical fluorescence spectra of three dysplastic patients, **c** typical fluorescence spectra of three normal volunteers, **d** typical spectra of cancerous patient, habitual and in-habitual volunteers



more than 5 to 6 times a day for the last 10 years), and an inhabited volunteer (consuming once or twice in a day for the couple of years) are shown in Fig. 3d. Enhancement of the fluorescence intensities of porphyrin bands with the progress of cancer (normal  $\rightarrow$  dysplasia  $\rightarrow$  OSCC) indicates that concentration of porphyrin increases with the progress of disease, which is reflected in the fluorescence spectra. However, spectral profiles of OSCC and dysplastic patients show that it is not always true that the intensities of porphyrin bands will always be dominant over the FAD band in all the cases. Therefore, analyzing the data by choosing specific biomarkers will not be appropriate. In other words, the selection of entire spectra for the data analysis could be a good choice. OSCC and dysplastic patients show higher FAD intensity if the porphyrin band is not present.

### Data analysis

To differentiate among the groups, we took the maximum value of intensity of porphyrin bands from all three groups and applied ROC on it. We could differentiate the groups, i.e., OSCC to normal, dysplasia to normal, and OSCC to dysplasia, with sensitivity and specificity values of 98%, 83%, 77%, and 100%, 98%, and 81%, respectively. Obtained sensitivity values for the differentiation of dysplastic to normal and OSCC to dysplastic groups are insignificant. Further, we took entire fluorescence spectra for the data analysis. Recorded fluorescence data have a dimension of

700, and it was reduced to a lower dimensional data set by employing the principal component analysis (PCA). Dimension reduction was done by estimating the principal components (PCs) of the correlation matrix ( $700 \times 700$ ).

Further, principal component (PC) scores were computed by projecting the original data along the PCs. The first 10 PCs consist of 99% total variance, in which the first two PCs (PC1 and PC2) consist of a total of 91% variance and 1st three PCs consist of a total of 93% variance. It indicates that the significant information is in the first 3 to 4 PCs. Scatter plots in between 1st and 2nd PC scores and 1st three PC scores are displayed in Fig. 4a and b. It can be seen clearly in both the figures that data of the control group is well separated from the data of the other two groups. For the classification among the groups, a support vector machine (SVM) classifier is applied on 1st and 2nd PC scores and 1st and 3rd PC scores, respectively. Before using the SVM classifier on the PC scores, PC scores are segregated into training and testing sets. Around 70% of data are taken for training and 30% for testing. By incorporating different kernels in the SVM classifier, we classified the groups and computed the various diagnostic parameters such as accuracy, sensitivity, and specificity.

Scatter data plots of linear kernel-based SVM classifier applied on 1st and 2nd PC scores and 1st and 3rd PC scores are shown in Fig. 5a–d. The linear kernel-based SVM classifier demonstrates excellent sensitivity and specificity for OSCC to normal, dysplasia to normal, and OSCC to

**Fig. 4** Scatter plots of PC scores of normal, dysplastic, and OSCC groups. **a** Scatter plot in between 1st and 2nd PC scores. **b** Scatter plot among the first three PC scores

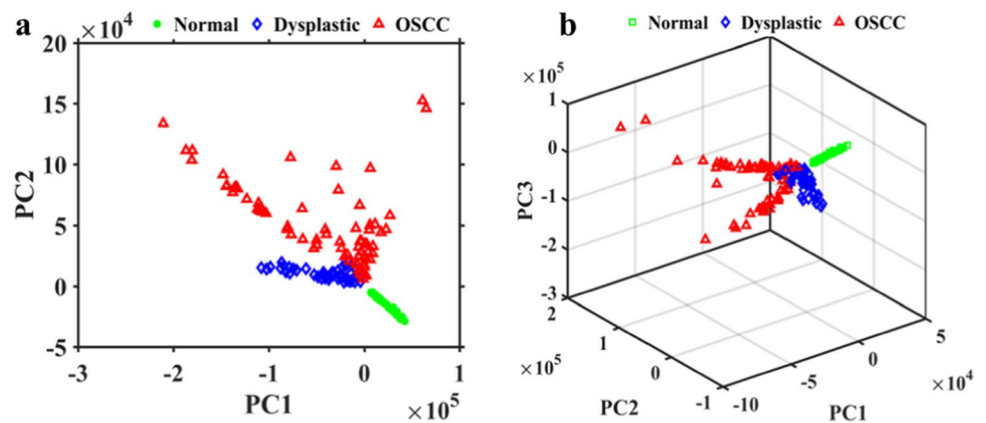
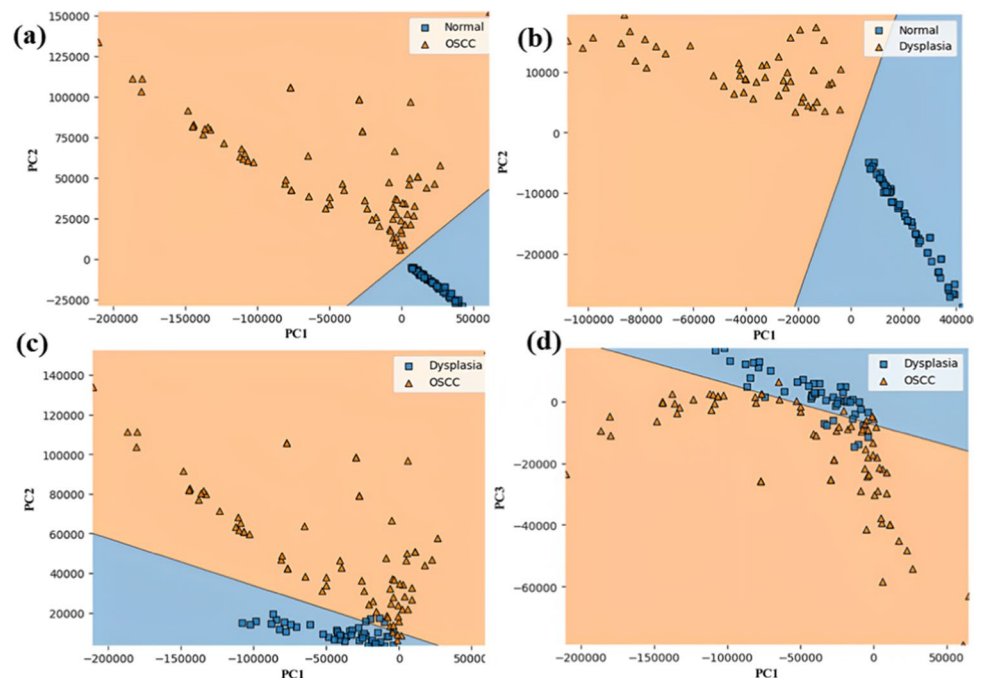


**Fig. 5** Linear-SVM-based classification on 1st three PC scores of **a** normal to OSCC data, **b** normal to dysplasia data, **c** dysplasia to OSCC data, **d** dysplasia to OSCC data



dysplasia with sensitivity values of 100%, 100%, and 95% and specificity values of 100%, 100%, and 94%, respectively. It is important to note that sensitivity and specificity values for discriminating OSCC to dysplasia are lower than 100%. Therefore, a linear SVM-based classifier on 1st and 3rd PC scores is applied but obtained fewer values than the previous values. Similarly, the RBF kernel was used on the data set, and diagnostic parameters were computed. Scatter data plots of RBF kernel-based SVM classifier applied on 1st and 2nd PC scores and 1st and 3rd PC scores are shown in Fig. 6a–d. Sensitivity and specificity values were found 100% among OSCC to normal and dysplasia to normal. RBF-SVM-based kernel could differentiate OSCC to dysplasia with sensitivity of 97% and 100%, respectively. RBF-SVM-based kernel applied on 1st PC and 3rd PC scores was also unable to discriminate the groups with 100% sensitivity values. Other kernels implemented in SVM, i.e., polynomial-SVM and

sigmoid-SVM-based, could not differentiate among the groups with significantly higher sensitivity and specificity values as the linear and RBF-based kernels did. The diagnostic values obtained among the groups from all the kernels are summarized in Tables 1 and 2. The process of picking training and testing datasets has been iterated multiple times, yielding consistent sensitivity and specificity values without significant variations.

## Conclusion

This clinical research aimed to detect and discriminate the oral mucosal lesions using the fluorescence-based portable device and support vector machine (SVM) classifier. To detect the oral mucosal lesions, we used an in-house developed device and performed measurements on patients

**Fig. 6** RBF-SVM-based classification on 1st three PC scores of **a** normal to OSCC data, **b** normal to dysplasia data, **c** dysplasia to OSCC data, **d** dysplasia to OSCC data

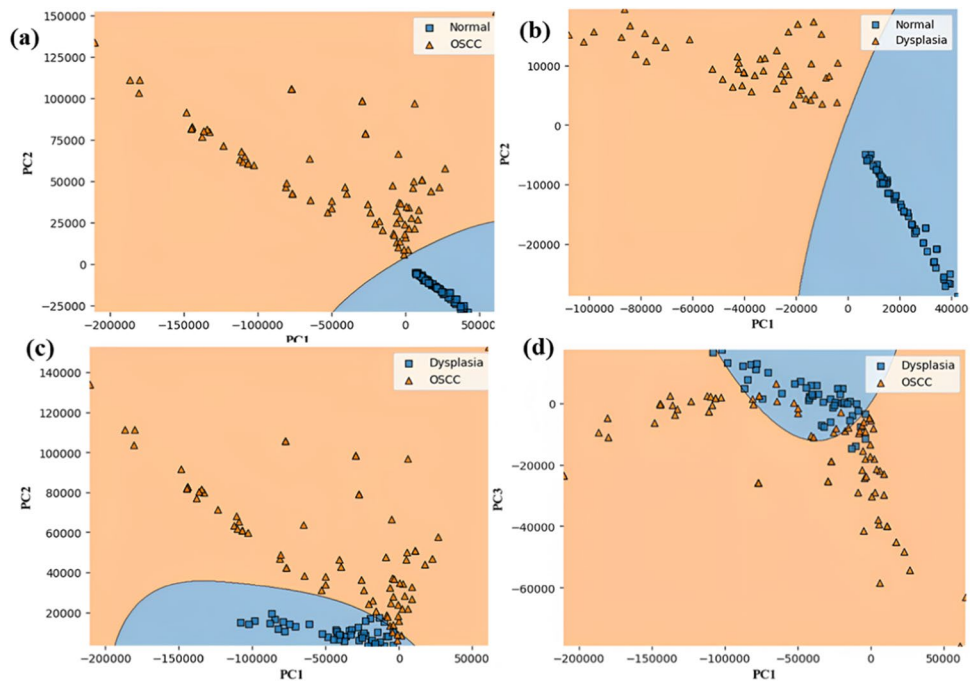


**Table 1** Sensitivity, specificity, and accuracy values for the testing data among the groups for linear and RBF kernels

Kernels→ Groups↓	Linear			RBF		
	Sensitivity	Specificity	Accuracy	Sensitivity	Specificity	Accuracy
OSCC/normal	100%	100%	100%	100%	100%	100%
Dysplasia/normal	100%	100%	100%	100%	100%	100%
OSCC/dysplasia	95%	94%	95%	95%	100%	97%

**Table 2** Sensitivity, specificity, and accuracy values for the testing data among the groups for polynomial and sigmoid kernels

Kernels→ Groups↓	Polynomial			Sigmoid		
	Sensitivity	Specificity	Accuracy	Sensitivity	Specificity	Accuracy
OSCC/normal	73%	100%	88%	100%	100%	100%
Dysplasia/normal	67%	100%	85%	100%	100%	100%
OSCC/dysplasia	100%	19%	67%	61%	37%	51%

(OSCC and dysplastic) and control groups. Measurements performed on 189 tissue sites of 81 patients and volunteers displayed two significant bands of FAD and porphyrin in the fluorescence spectra near 500 nm and at 634 nm, with some minor bands at 676 and 703 nm. The intensity of the porphyrin band was found much higher in OSCC and dysplastic patients than in normal volunteers. We found the accuracy values of 99%, 92%, and 79% by applying ROC on maximum values of porphyrin bands in all the three groups.

Further, we took the entire spectra of all three groups and reduced the dimension by employing PCA. We selected the first three PC scores and applied SVM on 1st and 2nd PCs and 1st and 3rd PCs, respectively. Before applying SVM on PC scores, the data set was divided into training and testing sets. Different kernels were included while analyzing the

data using the SVM. Linear and RBF-based kernels on 1st two PC scores were able to differentiate among the groups (OSCC to normal and dysplasia to normal) with 100% sensitivity and specificity and OSCC to dysplasia with sensitivity of 95% and 96% and specificity of 97% and 100%, respectively. Polynomial and sigmoid kernels implemented on SVM could differentiate the groups with the accuracy values of 56%, 76%, 88% 56%, 76%, and 88%, respectively. Linear and RBF could discriminate the groups with higher accuracy values out of the four kernels. Results displayed that RBF-SVM-based classification is comparable to linear-SVM. In conclusion, the hand-held device combined with a machine learning tool (PCA-SVM) may be a reliable screening method for the detection of oral mucosal lesions.

**Acknowledgements** I would like to acknowledge Dr. Surendra Kumar Kanaujia, who is the ENT specialist at GSVM Medical College Kanpur, UP, India

**Author contribution** Three authors have contributed in the manuscript. Dr. PK, who is the first and corresponding author, has done device fabrication, measurements, PCA, and ROC data analysis. Analysis by SVM is done by Dr. SR. The first draft of the manuscript is written by Dr. PK, and further modification was done by both of us. Dr. AP has helped in the fabrication of the device.

**Funding** We do not have any funding source. Biophotonics lab (SL-111) facilities in the Physics department at IIT Kanpur are utilized to conduct the research.

**Data availability** We do not have any objection on this point.

**Code availability** The authors have utilized Matlab and Python tools.

## Declarations

**Ethics approval** Ethical approval from the IIT Kanpur and GSVM Medical College committee members was taken before starting this clinical work. It is according to the Declaration of Helsinki.

**Consent to participate** We took informed consent from patients and volunteers.

**Consent for publication** The authors have agreed to publish.

**Conflict of interest** The authors declare no competing interests.

## References

- Chaturvedi AK, Anderson WF, Tieulent JL et al (2013) World-wide trends in incidence rates for oral cavity and oropharyngeal cancers. *J Clin Oncol* 31(36):4550–4559
- Ferlay J, Soerjomataram I, Dikshit R et al (2015) Cancer incidence and mortality worldwide: sources, methods and major patterns in globocan. *Int J Cancer* 136(5):359–386
- El-Naggar AK, Chan JKC, Takata T, Grandis JR, Slootweg PJ (2017) The fourth edition of the head and neck World Health Organization blue book: editors' perspectives. *Human Pathol* 66:10–12
- Scully C, Bagan JV, Hopper C, Epstein JB (2008) Oral cancer: current and future diagnostic techniques. *Am J Dent* 21:199–209
- Omar E (2015) Current concepts and future of noninvasive procedures for diagnosing oral squamous cell carcinoma—a systematic review. *Head Face Med* 11:1–27
- Patton LL, Epstein JB, Kerr AR (2008) Adjunctive techniques for oral cancer examination and lesion diagnosis: a systematic review of the literature. *J Am Dent Assoc* 139:896–905
- Farwell DG, Meier JD, Park J et al (2010) Time-resolved fluorescence spectroscopy as a diagnostic technique of oral carcinoma. *Arch Otolaryngol Head Neck Surg* 136:126–133
- Hillemanns P, Reiff J, Stepp H, Soergel P (2007) Lymph node metastasis detection of ovarian cancer by porphyrin fluorescence photo detection: case report. *Lasers Med Sci* 22:131–135
- De Veld DC, Bakker Schut TC, Skurichina M et al (2005) Auto fluorescence and Raman micro spectroscopy of tissue sections of oral lesions. *Lasers Med Sci* 19:203–209
- Bergholt MS, Zheng W, Lin K et al (2011) Combining near-infrared-excited auto fluorescence and Raman spectroscopy improves in vivo diagnosis of gastric cancer. *Biosens Bioelectron* 26:4104–4110
- Alfano RR (2012) Advances in ultrafast time resolved fluorescence physics for cancer detection in optical biopsy. *AIP Adv* 2:011103
- Singh SP, Deshmukh A, Chaturvedi P, Murali KC (2012) In vivo Raman spectroscopic identification of premalignant lesions in oral buccal mucosa. *J Biomed Opt* 17:105002
- DeCoro M, Wilder-Smith P (2010) Potential of optical coherence tomography for early diagnosis of oral malignancies. *Expert Rev Anticancer Ther* 10:321–329
- Onizawa K, Okamura N, Saginoya H, Yoshida H (2003) Characterization of auto fluorescence in oral squamous cell carcinoma. *Oral Oncol* 39:150–156
- Paderni C, Compilato D, Carinci F et al (2011) Direct visualization of oral-cavity tissue fluorescence as novel aid for early oral cancer diagnosis and potentially malignant disorders monitoring. *Int J Immunopathol Pharmacol* 24:121–128
- Goujon D, Zellweger M, Radu A, Grosjean P, Weber BC, van den Bergh H, Monnier P, Wagnieres G (2013) In vivo autofluorescence imaging of early cancers in the human tracheobronchial tree with a spectrally optimized system. *J Biomed Opt* 8:17–25
- Reichert D, Erkkilae MT, Gesperger J, Wadiura LI, Lang A, Roetzer T (2021) Fluorescence lifetime imaging and spectroscopic co-validation for protoporphyrin IX-guided tumor visualization in neurosurgery. *Front Oncol* 11:741303
- Amelink A, Sterenborg HJ, Roodenburg JL, Witjes MJ (2011) Non-invasive measurement of the microvascular properties of non-dysplastic and dysplastic oral leukoplakias by use of optical spectroscopy. *Oral Oncol* 47:1165–1170
- Betz CS, Stepp H, Janda P et al (2002) A comparative study of normal inspection, auto fluorescence and 5-ALA-induced PPIX fluorescence for oral cancer diagnosis. *Int J Cancer* 97:245–252
- Rahman MS, Ingole N, Roblyer D et al (2010) Evaluation of a low-cost, portable imaging system for early detection of oral cancer. *Head Neck Oncol* 2:10
- Roblyer D, Kurachi C, Stepanek V et al (2009) Objective detection and delineation of oral neoplasia using autofluorescence imaging. *Cancer Prev Res (Phila)* 2:423–431
- Policard A (1924) Etudes sur les aspects offerts par des tumeurs experimentales examinee a la lumiere de Woods. *C R Soc Biol (Paris)* 91:1423–1424
- Inaguma M, Hashimoto K (1999) Porphyrin-like fluorescence in oral cancer: in vivo fluorescence spectral characterization of lesions by use of a near-ultraviolet excited auto fluorescence diagnosis system and separation of fluorescent extracts by capillary electrophoresis. *Cancer* 86:2201–2211
- Gillenwater A et al (1998) Noninvasive diagnosis of oral neoplastic based on fluorescence spectroscopy and native tissue autofluorescence. *Arch Otolaryngol Head Neck Surg* 124:1251–1258
- Majumdar SK et al (2000) A pilot study on the use of auto fluorescence for diagnosis of the cancer of human oral cavity. *Curr Sci* 79:1089–1094
- Lane PM, Gilhuly T, Whitehead P, Zeng H, Poh C, Ng S, Williams M, Zhang L, Rosin M, MacAulay CE (2006) Simple device for the direct visualization of oral-cavity tissue fluorescence. *J Biomed Opt* 11:024006
- De Veld DC, Witjes MJ, Sterenborg HJ, Roodenburg JL (2005) The status of in vivo auto fluorescence spectroscopy and imaging for oral oncology. *Oral Oncol* 41:117–131
- Jayanthi JL, Subhash N, Stephen M, Philip EK, Beena VT (2011) Comparative evaluation of the diagnostic performance of autofluorescence and diffuse reflectance in oral cancer detection: a clinical study. *Biophotonics* 4:696–706



29. Nazeer SS et al (2014) Noninvasive assessment of the risk of tobacco abuse in oral mucosa using fluorescence spectroscopy: a clinical approach. *J Biomed Opt* 19:057013
30. Kumar P, Kanaujia SK, Singh A, Pradhan A (2019) In vivo detection of oral precancer using a fluorescence-based, in-house-fabricated device: a Mahalanobis distance-based classification. *Lasers Med Sci* 34:1243–1251
31. Betz CS, Mehlmann M, Rick K et al (1999) Autofluorescence imaging and spectroscopy of normal and malignant mucosa in patients with head and neck cancer. *Lasers Surg Med* 25:323–334
32. Van Staveren HJ, van Veen RL, Speelman OC et al (2000) Classification of clinical autofluorescence spectra of oral leukoplakia using an artificial neural network: a pilot study. *Oral Oncol* 36:286–293
33. Sah AN, Kumar P, Pradhan A (2023) In vivo testing of oral mucosal lesions with in-house developed portable imaging device and comparison with the spectroscopy results. *J Flu* 26:1–9
34. Wu JY, Yi C, Chung HR et al (2010) Potential biomarkers in saliva for oral squamous cell carcinoma. *Oral Oncol* 46:226–231
35. Kumar P, Singh A, Kanaujia SK, Pradhan A (2018) Human saliva for oral precancer detection: a comparison of fluorescence & stokes shift spectroscopy. *J Fluoresc* 28:419–426
36. Kumar P (2022) Detection of inaccessible head and neck lesions using human saliva and fluorescence spectroscopy. *Lasers Med Sci* 37:1821–1827
37. Sahoo GR, Singh P, Pandey K, Kala C, Pradhan A (2018) Improving diagnosis of cervical pre-cancer: combination of PCA and SVM applied on fluorescence lifetime images. In *Photonics* 5(4):57
38. Thapa P, Singh V, Kumar V, et al. (2022) Multimodal optical techniques in pre-clinical evaluation of oral cancer: fluorescence imaging and spectroscopic devices. arXiv preprint arXiv:2211.05230.
39. Fawcett T (2006) An introduction to ROC analysis. *Pattern Recognit Lett* 27:861–874
40. Kumar P, Pradhan A (2023) Human saliva as a substitute diagnostic medium for the detection of oral lesions using the stokes shift spectroscopy: discrimination among the groups by multivariate analysis methods. *Asian Pacific J Cancer Prev: APJCP* 24(11):3757–3763

**Publisher's Note** Springer Nature remains neutral with regard to jurisdictional claims in published maps and institutional affiliations.

Springer Nature or its licensor (e.g. a society or other partner) holds exclusive rights to this article under a publishing agreement with the author(s) or other rightsholder(s); author self-archiving of the accepted manuscript version of this article is solely governed by the terms of such publishing agreement and applicable law.